A probabilistic model of rainfall-triggered shallow landslides in hollows: A long-term analysis

Paolo D'Odorico

Department of Environmental Sciences, University of Virginia, Charlottesville, Virginia, USA

Sergio Fagherazzi

Department of Geological Sciences and School of Computational Science and Information Technology, Florida State University, Tallahassee, Florida, USA

Received 18 July 2002; revised 1 June 2003; accepted 27 June 2003; published 18 September 2003.

[1] The long-term temporal evolution of soil thickness in hollows depends on the processes controlling the rates of colluvium accumulation and erosion. Accumulation is due to soil creep and mass-wasting processes from the adjacent slopes, while erosion of colluvial deposits is mainly due to debris flow and landsliding. An analysis of the long-term evolution of colluvial deposits is developed through a stochastic model of soil mass balance at a point accounting for colluvium infilling, expressed as a deterministic function of the deposit thickness, and soil erosion by shallow landslides, modeled as a random (Poisson) process. Landsliding is related to the characteristics of the triggering precipitation through an infinite-slope stability analysis, a kinematic model of hollow response to rainfall, and the intensity-duration-frequency curves characterizing the regime of extreme precipitation. This analysis provides a probabilistic representation of the long-term dynamics at a point of colluvium thickness as a function of the timescale of hollow infilling and of the frequency of triggering rainfalls. The model is solved both numerically and (under simplified conditions) analytically, showing the existence of different regimes in the temporal evolution of soil thickness. In the case of steep slopes (i.e., with slope angles, β, greater than the soil repose angle, ϕ) the hollow can be either in a supply-limited state or in event-limited conditions, depending on whether the dynamics are limited by the supply of sediment from the adjacent slopes or by the occurrence of rainstorms able to trigger landslides. Nevertheless, since the likelihood of landslide occurrence increases with increasing values of deposit thickness, colluvium accretion always leads to conditions favorable to landsliding. Vice versa, in the case of gentle slopes (i.e., $\beta < \phi$) the probability of landsliding decreases with increasing values of soil thickness, and event-limited conditions may evolve into unconditionally stable states. *INDEX TERMS:* 1625 Global Change: Geomorphology and weathering (1824, 1886); 1869 Hydrology: Stochastic processes; 1854 Hydrology: Precipitation (3354); *KEYWORDS:* landslide, hollow hydrology, soil thickness, landscape evolution, rainfall

Citation: D'Odorico, P., and S. Fagherazzi, A probabilistic model of rainfall-triggered shallow landslides in hollows: A long-term analysis, *Water Resour. Res.*, *39*(9), 1262, doi:10.1029/2002WR001595, 2003.

1. Introduction

[2] The temporal evolution of regolith and colluvial deposits in hollows is the result of nonlinear dynamics [*Minasny and McBratney*, 1999] involving several hydrological, geomorphological, and climatologic factors. In steep, soil mantled landscapes, landslides triggered by heavy rain remove colluvium, whereas transport of soil from the adjacent slopes (by means of soil creep, animal burrowing, tree throw, and rainwash [e.g., *Dietrich et al.*, 1987; *Roering et al.*, 1999]) and weathering of the underlying bedrock contribute to hollow infilling. Colluvial deposits in hollows are generally subject to more frequent landsliding than convex ridges due to the convergent topography and the consequently high concentrations of water and sediment fluxes [e.g., *Dietrich et al.*, 1986; *Sidle*, 1987; *Reneau and Dietrich*, 1987; *Reneau et al.*, 1989; *Crozier et al.*, 1990].

[3] Some authors [e.g., *Wu and Swanston*, 1980; *Dunne*, 1991; *Benda and Dunne*, 1997; *Iida*, 1999; *Lancaster et al.*, 2001] suggest that because of their abrupt and random character, landslides need to be modeled as discontinuous stochastic processes. Thus the temporal evolution of colluvial deposits in hollows can be characterized by a continuous process of deposit accretion, and a discontinuous random process of denudation caused by rainfall-triggered landslides and debris flow, which scour to bedrock large portions of the hollow. The temporal evolution of colluvium thickness can thus be studied through a stochastic soil mass balance, accounting for the supply of debris from the adjacent slopes and for random denudation

0043-1397/03/2002WR001595$09.00

due to landsliding. A number of studies analyze the soil mass balance to investigate the spatial and temporal patterns of soil thickness. This approach has led to models of equilibrium profiles in hillslopes [*Kirkby*, 1971; *Carson and Kirkby*, 1972], of landform evolution [*Ahnert*, 1988], as well as of the spatial variability of regolith thickness in soil-mantled landscapes [*Dietrich et al.*, 1995; *Heimsath et al.*, 2001].

[4] Two recent contributions have explored in detail the linkage between rainstorm characteristics and landslide frequency [*Benda and Dunne*, 1997; *Iida*, 1999]. In the work of *Benda and Dunne* [1997] [see also *Dunne*, 1991] the soil mass balance in hollows is studied through a numerical model accounting for the random character of both precipitation and forest fires. Their model suggests an interesting approach to determine the sediment supply to the channel network: it accounts for the process of colluvium accretion, and for the conditions of slope stability, including the reinforcement effect of roots. The latter is expressed as a function of deposit thickness and fire occurrence. In the hydrologic portion of the model, the peak saturated thickness is estimated as a function of randomly generated values of storm duration and intensity derived from exponential distributions. However, the storm characteristics are not related to the intensity-duration-frequency curves characterizing the regime of extreme precipitation. Thus the link between storm intensity, duration, and return period is missing and this approach provides neither an analysis of the probability distribution of the frequency of triggering precipitation, nor a comparison between the timescale of hollow infilling and the return period of the triggering rainfall. A similar stochastic approach, based on the rainfall model by *Eagleson* [1978], is used in models focusing on the influence of the rainfall regime on landslides, soil mass-wasting processes, and landscape evolution [*Tucker and Bras*, 2000; *Lancaster et al.*, 2001; *Tucker et al.*, 2001]. These papers lay the foundations of the stochastic analysis of landscape evolution.

[5] Fundamental in this direction is the stochastic model developed by *Iida* [1999], where the frequency of landslide occurrence is related to the return period of those rainstorms that are able to exceed limit-equilibrium conditions. The assessment of slope stability refers to the concept of immunity depth, defined as the minimum value of colluvium thickness required for the occurrence of landslides. The role of the immunity depth, derived directly from the soil stability model, becomes crucial in assessing the return period of the triggering rainfalls, thus influencing the stochastic analysis of landsliding. Moreover, the analysis of soil stability in terms of soil thickness (immunity depth and maximum depth, defined in the following sections) rather than soil characteristics (repose angle and cohesion, both difficult to measure in the field) introduces parameters that the author is able to determine directly using field data. This model accounts for the mutual dependence between rainstorm duration and intensity, and relates the return period and scar depth to the characteristics of extreme precipitation as well as to the rates of soil development. However, this approach does not explicitly analyze a soil mass balance, and does not provide the probability distribution of the colluvium depth.

[6] A simplified framework has already been suggested [*D'Odorico*, 2000; *D'Odorico et al.*, 2001] for the study of soil depth probability distribution in hillslopes. In this paper a similar mechanistic approach is utilized for the analysis of landsliding in hollows: the process of colluvium accretion is expressed as a function of diffusion-like transport [*Dietrich et al.*, 1986] from the adjacent slopes, while landslide occurrence is modeled at a point as a stochastic process of Poissonian [*Wu and Swanston*, 1980] events that completely scour the colluvium to bedrock. The assumption of complete removal of regolith by landslides is supported by some observational evidence that the failure surface generally coincides with the regolith-bedrock interface [e.g., *O'Loughlin and Pearce*, 1976; *Sidle and Swanston*, 1982; *Trustrum and De Rose*, 1988].

[7] Our model accounts for the mutual dependence between intensity, duration, and frequency of extreme precipitation [see *Caine*, 1980]. The coupling of storm-frequency analysis with a simple model of hollow response to precipitation relates landslide return period to the frequency of triggering precipitation. The slope stability portion of the model refers to the immunity depth concept [*Iida*, 1999] and shows its significance to the temporal evolution of colluvium thickness. The limited number of parameters required by this simplified framework favors an analysis of how landsliding is affected by the different hydrologic, geomorphic, and geomechanical variables. The framework introduced by *Iida* [1999], and in particular the concept of immunity depth, is then extended to hollow angles less than the repose angle of the material.

[8] Because of the random character of landsliding the deposit thickness needs to be considered as a random variable: Thus the properties of the colluvium depth are expressed in terms of probability distributions of soil depth at a point. This probabilistic framework is instrumental to the study of different regimes of hollow dynamics and to the understanding of their dependence on different hydrologic and geomorphic parameters. Moreover, the estimation of the probability distribution of landslide thickness and return period allows for the evaluation of the long-term average rate of sediment supply to the channel network as well as the assessment, in the use of cosmogenic nuclides methods [e.g., *Heimsath et al.*, 1997, 2001], of the probability that the existing deposit depth coincides with the long-term average soil thickness under which the observed nuclide accumulated.

[9] Finally, the introduction of a suitable potential function sheds light on the preferential states of the system and the derivation of analytical results, under simplified conditions, allows a direct calculation of the thickness distribution of colluvial deposits.

2. Slope Stability Model

[10] In the characterization of landslide frequency a soil mass balance needs to be studied in time and related to the processes affecting colluvium deposition, soil stability, and hollow hydrology. The soil stability model used in this study is based on a Mohr-Coulomb failure law applied to an infinite planar slope [*Terzaghi and Peck*, 1967]. The assumption of infinite planar slope, extensively utilized in geomorphic studies [e.g., *O'Loughlin and Pearce*, 1976; *Wu et al.*, 1979; *Wu and Swanston*, 1980; *Sidle and Swanston*, 1982; *Selby*, 1983; *Montgomery and Dietrich*,

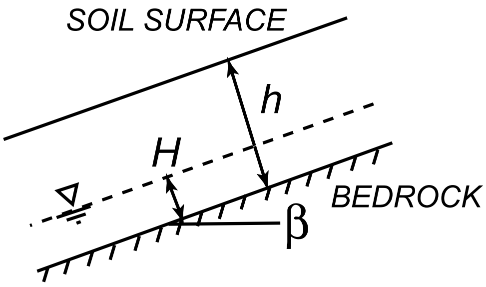

Figure 1. Schematic representation of a soil-mantled slope.

1994; *Dietrich et al.*, 1995; *Iida*, 1999; *Iverson*, 2000], represents a good approximation when the soil thickness is small with respect to the length of the slope. More accurate models would not be justified, due to the lack of knowledge on the soil geotechnical and hydrological properties as well as of their spatial variability [e.g., *Sidle et al.*, 1985]. The failure condition can be expressed as [*Montgomery and Dietrich*, 1994]:

$$\gamma_{sat} h \sin\beta = c + (\gamma_{sat} h \cos\beta - \gamma_w H \cos\beta) \tan\phi \qquad (1)$$

where γ_{sat} and γ_w are the specific weights of saturated soil and water, respectively; β is the slope angle, ϕ is the soil repose angle, c the soil cohesion, h the soil thickness, and H the saturated water depth, with both H and h being measured perpendicularly to the bedrock (Figure 1). In (1) it is considered that the subsurface flow is uniform with hydraulic gradient corresponding to the topographic slope. Equation (1), solved for H, provides the minimum value of landslide-triggering saturated depth:

$$H = \frac{\gamma_{sat}}{\gamma_w} h \left(1 - \frac{\tan\beta}{\tan\phi}\right) + \frac{c}{\gamma_w \tan\phi \cos\beta}. \qquad (2)$$

Equation (1) expresses how the stability or instability of a slope depends on slope angle and soil thickness. The colluvium thickness for which $H = h$ is defined as immunity depth [e.g., *Iida*, 1999]

$$h_{cr} = \frac{c}{\gamma_w \tan\phi \cos\beta + \gamma_{sat} \cos\beta (\tan\beta - \tan\phi)}. \qquad (3)$$

Because saturated depth is necessarily smaller than colluvium thickness (i.e., $H \leq h$), when $h < h_{cr}$ the deposit is always stable (according to this model) independently of rainfall intensity. After landsliding, soil mass-wasting from the surrounding slopes accumulates new colluvium in the hollow and the deposit is not susceptible to failure until its thickness reaches h_{cr}. This early stage of colluvium accretion (i.e., for $h < h_{cr}$) is termed immunity period (T_{imm}).

[11] Figure 2 shows different conditions of slope stability in a plot of soil thickness versus slope. The angle β_0 represents the value of β cancelling the denominator of (3); according to this model, when $\beta < \beta_0$ the slope is always stable because a saturated depth larger than the soil thickness would be needed to trigger a landslide. Other destabilizing factors, which are not part of this model (e.g., excess of pore pressure), can trigger landslides even when $\beta < \beta_0$. For $\beta > \beta_0$ the colluvium can be stable or unstable depending on whether the soil depth exceeds the immunity depth. For $\beta = \beta_0$ the immunity depth is infinite, and it decreases with increasing values of β when $\beta > \beta_0$. Equation (2) shows that the saturation depth, H, needed for landslide triggering increases linearly with the soil thickness for slope angles less than the repose angle ($\beta < \phi$), while it linearly decreases with h for $\beta > \phi$. The reason for this different dependence can be found in the analysis of the components (normal and parallel to bedrock) of the soil weight. In the case of $\beta < \phi$, the overall effect of soil weight is to favor the slope stability; vice versa for $\beta > \phi$ an increase in soil mass favors instability.

[12] From a hydrological viewpoint, for $\beta < \phi$, the accumulation of colluvium in the hollow increases the storm intensity needed for landslide triggering. Conversely, for $\beta > \phi$, an increase in deposit thickness due to colluvium accumulation in the hollow is associated with a decrease of the intensity of the storms that are able to generate a landslide. For a certain value of soil thickness, h_{max}, the saturated depth necessary to trigger a landslide is zero and the soil is always unstable, regardless of rainfall occurrence [*Iida*, 1999]. For soil thickness higher than h_{max} the soil is then always unstable (see Figure 2); h_{max} is determined from (2) by setting $H = 0$.

$$h_{max} = \frac{c}{\gamma_{sat} \cos\beta (\tan\beta - \tan\phi)} \qquad (4)$$

[13] When cohesion is neglected (i.e., $c = 0$ in equation (1)), the immunity depth is zero and, for $\beta > \phi$, the soil is always unstable because cohesion is not preventing landslide occurrence. Soil cohesion has been sometimes neglected in the stability analyses of steep mantled slopes, while the repose angle has been purposely increased to unrealistic values to account for the overall shear strength of the aggregates [e.g., *Montgomery and Dietrich*, 1994]. Even though this approach is effective in the analysis of the spatial distribution of landsliding, it is not suitable for the study of the temporal evolution of soil thickness

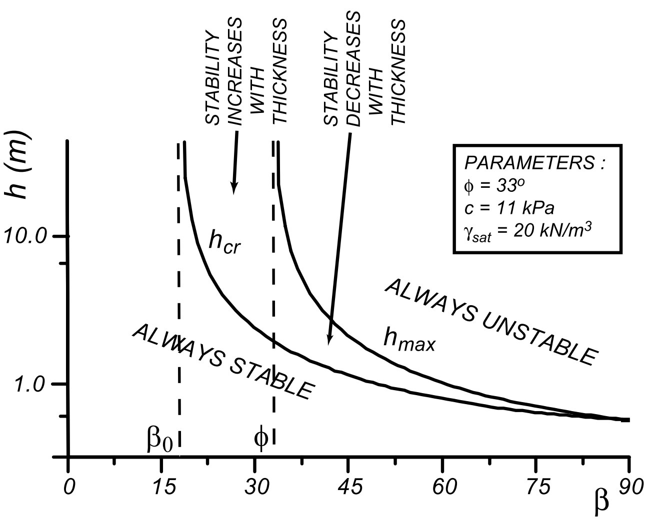

Figure 2. Slope stability as a function of slope angle and deposit thickness (equations (3) and (4)).

because it does not include the immunity depth as a threshold controlling landslide occurrence. The implications for modeling soil evolution are important because without cohesion soils could never form on slopes greater than ϕ and even thin soils on slopes in the range $\beta_0 < \beta < \phi$ would be extremely unstable since light (i.e., frequent) rainfall would provide a saturated water depth H sufficient to cause landslides. Both these implications are contrary to observation and suggest that soil cohesion (and hence the concept of immunity depth) are needed in slope stability models.

3. Hydrologic Model

[14] The coupling of the soil stability model presented in the previous section with a hydrologic model for hollow response to precipitation allows the determination of the rainfall characteristics (i.e., intensity and duration) associated with the occurrence of landsliding. A simplified yet effective model has already been used to study the spatial distribution of landsliding [*Montgomery and Dietrich*, 1994; *Dietrich et al.*, 1995; *Montgomery et al.*, 1998], assuming that hollows respond to rainstorms with a steady subsurface flow. The saturated depth is determined through a steady state water balance equation for the hollow. The incoming flux (precipitation) is equated to the outgoing subsurface flow occurring through the saturated depth, $RA = HK_s b \sin\beta$, where R is the (constant) rainfall intensity, K_s is the soil hydraulic conductivity, $K_s \sin\beta$ is the specific discharge of the subsurface flow (Darcy's law in the assumption of uniform flow), A represents the contributing area to the failure point, and b the width of the hollow boundary at the downhill side. The saturated depth can be then expressed [*O'Loughlin*, 1986] as

$$H = \frac{RA}{K_s b \sin\beta} \tag{5}$$

Notice that this steady state model does not provide any information on rainfall duration. Nevertheless, the triggering precipitation needs to be characterized both in terms of storm intensity and duration. In fact, the analysis of landslide frequency requires the estimation of the return period of the triggering rainfall through the intensity-duration-frequency (IDF) curves. To this end, the rational method [e.g., *Chow et al.*, 1988] is applied to the subsurface flow in the hollow to determine the most critical storm duration, i.e., the duration of the storms that, for a given return period, produces the highest values of H. This method represents one of the simplest conceptual models of basin response and is here applied to the subsurface water flow in hollows. The rational method refers to the concept of concentration time, T_c, defined as the travel time in the subsurface flow between the furthermost point in the hollow and the hollow outlet. The rational method assumes that T_c is the most critical storm duration. In fact, for durations shorter than T_c the hollow is never entirely contributing to the flow (and to the related water depth, H, at the outlet) because the contributing area is always smaller than A. On the other hand, since for a given return period rainfall intensity decreases with the duration, the concentration time is the duration of the most intense storm associated with the maximum contributing area (i.e., A). Thus the maximum saturated depth generated by storms of a given frequency is due to events of duration T_c. Of course landslides can be triggered also by events shorter than T_c (i.e., with only partial contributing areas) with high rainfall rates. The framework of the rational method is used here only to determine the duration and intensity of the most critical storm (i.e., storm with lowest return period able to cause a landslide). The concentration time can be expressed through the ratio between the length of the longest drainage path and the specific discharge of the subsurface flow

$$T_c = C\frac{\sqrt{A}}{K_s \sin\beta}, \tag{6}$$

where the longest path is expressed as a function of the square root of the hollow contributing area, $\sqrt{A}$, and C is a (dimensionless) coefficient accounting for other factors affecting the concentration time (e.g., heterogeneity in soil properties, hollow shape, etc.). Equation (6) assumes that $\sqrt{A}$ is an appropriate scale for hollow length. Moreover, the celerity of the response wave propagation through the hollow is expressed as proportional to the specific discharge of the subsurface flow with hydraulic gradient equal to the topographic slope; the proportionality constant is buried in C. The characteristics of the triggering precipitation are expressed by (6) and by (5) with H being given by (2). This implies that R (i.e., the minimum rainfall intensity needed to trigger a landslide) is a function of h.

4. Frequency of the Triggering Precipitation

[15] Given the rainfall intensity and duration, the return period of the rainstorms able to trigger landslides is derived from the IDF curves. Since landslides are triggered by extreme rainfalls, we use a Gumbel distribution [e.g., *Chow et al.*, 1988] to express the dependence between annual maximum rainfall intensity (for events of duration T_c), and return period, T_r

$$\frac{1}{T_r} = \lambda = 1 - \exp\left[-\exp\left(-\frac{R(T_c) - u}{v}\right)\right] \tag{7}$$

where T_r is the return period, $R(T_c)$ is the maximum rainfall intensity of duration T_c, u and v are the parameters of the Gumbel distribution, λ is the probability that a rainstorm of intensity R occurs in a given year; u and v can be determined as functions of the mean, μ_R, and variance, σ_R^2, of R ($u = \mu_R - 0.577\sigma_R$; $v = 0.779\sigma_R$). Thus, after having determined the concentration time, T_c, for the hollow in question, the parameters u and v can be estimated from the data of extreme precipitation of duration T_c. Notice how $\lambda = 1/T_r$ is a function of the soil depth due to the dependence existing between intensity of the triggering precipitation, R, and h (equation (5)).

5. Colluvium Infilling

[16] The growth of colluvial deposits in a hollow is due to the transport of soil from uphill as well as to the physical weathering of the underlying bedrock. The transport of debris from the surrounding hillslopes is caused by different mechanisms such as soil creep, animal burrowing, tree throw, rain splash, and overland flow and relies on the production of regolith as well as on the existence of a slope.

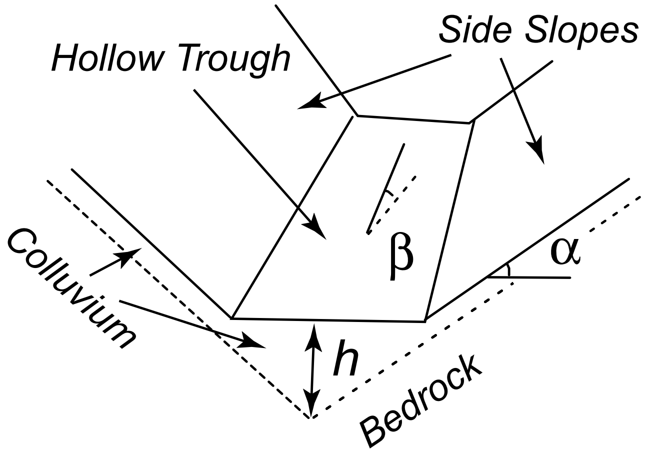

Figure 3. Schematic representation of regolith mantle and bedrock in a hollow (modified from *Dietrich et al.* [1986]).

The soil production by bedrock weathering is due to a number of chemical, physical, and biogenic processes [e.g., *Birkeland*, 1999]. In this paper we assume that soil production by bedrock weathering beneath the hollow is negligible with respect to soil accumulation due to diffusive processes [e.g., *Heimsath et al.*, 1997; *Anderson et al.*, 2002].

[17] The rate of transport to the hollow due to diffusion-like mass-wasting processes depends on the sediment flux at each point of the hillslope. For a hollow composed of a tipped triangular trough and two planar side slopes (Figure 3), *Dietrich et al.* [1986] expressed the accretion of colluvial deposits as:

$$h = \left[2D_c \cos\beta\left(\tan^2\alpha - \tan^2\beta\right)t\right]^{1/2} \tag{8}$$

where α is the angle between the side slopes and an horizontal plane, β is the slope angle of the colluvium-mantled hollow (Figure 3), and D_c is the soil creep diffusivity [*Culling*, 1960] (for a recent discussion regarding creep diffusivity and its dependence on soil thickness, see also *Furbish and Fagherazzi* [2001]).

[18] Starting from a condition $h = 0$ at time $t = 0$, the colluvium thickness increases proportionally to $\sqrt{t}$ (see (8)), due to the linear increase of trough cross-sectional area. Since α and β depend on the hollow geometry that - we assume - does not vary substantially with time, we can express (8) as:

$$h = \sqrt{Kt}; \quad K = 2D_c \cos\beta\left(\tan^2\alpha - \tan^2\beta\right) \tag{9}$$

with K being independent of time.

[19] The differentiation of (9) with respect to time leads to

$$\frac{dh}{dt} = l(h) = \frac{K}{2h}, \tag{10}$$

showing that the rate of colluvium accretion decreases with the depth, h, of the deposit.

6. Stochastic Soil Mass Balance

[20] The study of landslide occurrence and temporal dynamics of colluvial deposits requires an analysis of the processes responsible for the accumulation and removal of soil waste material in the hollow. The temporal evolution of the deposit thickness, h, can be modeled through the soil mass balance equation [e.g., *Carson and Kirkby*, 1972]:

$$\frac{dh}{dt} = l(h) - f(h,t) \tag{11}$$

where $l(h)$ is a state-dependent function of net colluvium accumulation expressed by (10) and $f(h,t)$ is the rate of soil removal by debris flow and shallow landslides. Because of the catastrophic and random nature of landsliding, the erosion function, $f(h,t)$, in equation (11) is modeled as a stochastic Poisson process. Rainstorms able to trigger landslides occur at random times t_i and remove the whole soil column h, as long as the deposit thickness exceeds the immunity depth:

$$f(h,t) = \omega(h)\sum_i \delta(t - t_i) \tag{12}$$

where

$$\omega(h) = \begin{cases} 0; & 0 \le h \le h_{cr} \\ h; & h > h_{cr}. \end{cases} \tag{13}$$

In equation (12), δ represents a δ-Dirac function and the sequence t_i ($i = 1, 2, \ldots$) is such that the recurrence interval of the triggering precipitation, $\tau = t_{i+1} - t_i$, is an exponentially distributed random variable as in *Wu and Swanston* [1980]; the probability density function of τ is thus $p(\tau) = \lambda\, e^{-\lambda\tau}$, with λ being the frequency of the triggering precipitation. Notice how λ (equation (7)) is state-dependent (i.e., $\lambda = \lambda(h)$) since the intensity, R, of the triggering precipitation depends on h through equations (5) and (2).

[21] Equations (10), (11), and (12) provide a representation of the dynamics of hollow infilling and erosion and incorporate the main relevant processes along with their mutual dependence and interaction. In fact, the temporal variability of colluvium thickness is controlled by the rates of colluvium accretion and erosion (i.e., landslides), and both of them depend on the actual state (i.e., deposit thickness) of the system. The model accounts for the randomness of landsliding, the regime of extreme precipitation (IDF curves), and the dependence on slope angle and soil mechanical properties (infinite-slope stability analysis). In the following sections the stochastic differential model (equations (10), (11), and (12)) is numerically solved providing a probabilistic analysis of deposit thickness, landslide depth, and landsliding frequency in a hollow. An analytical solution of these equations is then provided under some simplifying assumptions. Analytical and numerical solutions are finally compared.

7. Numerical Simulation of Hollow Dynamics

[22] After having determined the concentration time T_c of the hollow, the parameters u and v in (7) are estimated from data available on extreme precipitation of duration T_c. The stochastic model of colluvium infilling and landsliding (equation (11)) is then numerically resolved starting from

the initial condition $h = 0$ at time 0 (i.e., hollow scoured to bedrock); the following steps are performed with a time step, Δt, of one year: (1) Equation (2) is used to calculate the saturated water depth, H, able to trigger landslides with the existing soil thickness, h; (2) the rainfall intensity, R, corresponding to H is calculated using (5); (3) the probability $\lambda \Delta t$ of having a landslide-triggering event in the current year is calculated through equation (7); (4) a random number generated between 0 and 1 is compared to $\lambda \Delta t$ to simulate the random occurrence or nonoccurrence of the triggering rainstorm in that year. In the case that such a rainstorm occurs a landslide scours the hollow to bedrock only if the deposit thickness exceeds the immunity depth, otherwise no landslide occurs; (5) the soil thickness in the hollow is increased according to equation (10); (6) back to step 1 for the subsequent time step.

[23] The model simulates the temporal evolution of deposit thickness in time, determines the inter-arrival time between consecutive landslides as well as the depth of the landslide scar (defined as the colluvium thickness at the time of landslide occurrence).

8. Results and Discussion

8.1. Case of Steep Hollows ($\beta > \phi$)

[24] The model is applied to a parameter set derived from published data from the Oregon Coastal range. The conductivity K_s is taken as 65 m d^{-1}, the soil repose angle is $\phi = 33°$, while γ_{sat} = 20 kN m^{-3} [*Montgomery et al.*, 1998], the diffusivity coefficient for colluvium infilling $D_c = 0.0032$ m^2 yr^{-1} is the average value for bioturbation and soil creep transport rate in the Oregon Coastal range [*Benda and Dunne*, 1997; *Reneau et al.*, 1989]. A value of soil cohesion $c = 11$ kPa is adopted to account for the root effect in a mature forest [*Montgomery et al.*, 1998; *Benda and Dunne*, 1997]; we also assume a ratio between hollow gradient and side gradients (corresponding to $\tan\beta/\tan\alpha$ in equation (8)) equal to 0.8, as reported by *Dietrich et al.* [1986]. The consequences of forest fire and logging are not considered in this analysis, as well as the reduction of soil cohesion due to an increase in soil thickness. In our numerical analysis we refer to hollows having the same characteristics as the ones extensively studied by *Montgomery et al.* [1997], *Anderson et al.* [1997], and *Torres et al.* [1998]. The first hollow, the dimensions of which approximately correspond to the hollow CB2 of *Montgomery et al.* [1997], has a drainage area, A = 3700 m^2, the outlet width, b, is of about 12 m, and the hollow slope is $\beta = 43°$. Thus the immunity depth (equation (3)) is $h_{cr} = 1.24$ m. As discussed before, the fact that $\beta > \phi$ implies that the hollow becomes less stable as the deposit thickness increases. A coefficient $C = 0.38$ is determined from equation (6) using parameters (see the following example) available for the smaller hollow (CB1) of *Montgomery et al.* [1997]. If the same value of C is assumed for the hollow CB2, equation (6) gives a concentration time T_c = 12 h. Values of $u = 2.78$ mm h^{-1} and $v = 1.07$ mm h^{-1} have been calculated using data of extreme precipitation of 12 h duration from Alleghany (Oregon, 1951–2000).

[25] The rainfall intensity saturating the immunity depth, R_{cr}, in 12 hours is estimated through the hydrological model (5) and it is found to be $R_{cr} = 7.5$ mm h^{-1}. This value of R with duration $T_c = 12$ h has a return period, $1/\lambda(h_{cr}) = 90$ yrs (equation (7)). For values of h larger than the immunity depth the triggering rainfall decreases in intensity, with a consequent sharp reduction of the return period. The hollow has immunity period (i.e., time needed to accumulate a colluvium thickness $h = h_{cr}$), T_{imm} = 670 yr (from equation (9) with $h = h_{cr}$). If the accumulation of material in the hollow is very slow compared to the temporal interval between consecutive triggering storms (i.e., $T_{imm} \gg 1/\lambda(h_{cr})$) landslides occur soon after the thickness of the colluvial deposit reaches the immunity depth because a landslide-triggering storm will occur before the hollow is able to develop a colluvium much thicker than h_{cr}. The comparison between the timescale of hollow infilling (greater than 670 yr) and the return period of the triggering rainfall (90 yr) shows that this is the case for the hollow in question. Model results confirm this analysis: a plot of the time series of colluvium thickness (Figure 4a) shows how landslides occur with values of soil thickness slightly above the immunity depth. The probability distribution of landslide thickness is clustered around the immunity depth (Figure 4b) and the probability distribution of triggering rainfall return period and landslide return period are also concentrated close to $1/\lambda(h_{cr})$ and T_{imm}, respectively (Figures 4c and 4d). The probability distribution of soil depth sharply drops for values of h above the immunity depth (Figure 4e).

[26] In these conditions ($T_{imm} \gg 1/\lambda(h_{cr})$) landslide occurrence is limited by the supply of debris from the adjacent slopes and not by the occurrence of triggering precipitation: we denote this regime as "supply limited". Landslide return period, T_{slide}, and depth, h_{slide}, have a small variance since $T_{slide} \approx T_{imm}$, and $h_{slide} \approx h_{cr}$. The mode of the probability distribution of h is at $h = h_{cr}$.

[27] The occurrence of supply-limited conditions is common in landscapes having precipitation and rates of diffusion-like mass wasting comparable to those considered in this example [*Dietrich et al.*, 1995; *Benda and Dunne*, 1997]. Nevertheless, a substantial decrease of hollow slope (though still in the range $\beta > \phi$) or size is able to lead to "event-limited" conditions characterized by $1/\lambda(h_{cr}) \gg T_{imm}$. For example, in smaller hollows the smaller contributing area is associated with larger values of R (equation (5)). Thus landslides are triggered by less frequent events. As pointed out by *Montgomery and Dietrich* [1994], drainage area has a strong influence on slope stability, concentrating shallow landsliding in areas with convergent topography and larger contributing areas. Since less rainfall is concentrated at the hollow outlet, a higher rainfall intensity is necessary to trigger a landslide. Figure 5 shows the case of a hollow with the same characteristics as that of Figure 4 but with an area A = 860 m^2, corresponding to the hollow CB1 of *Montgomery et al.* [1997]. The values of h_{cr}, h_{max}, and T_{imm} remain unchanged, while T_c = 6 h and R_{cr} is 15.9 mm/h. This value of T_c corresponds to the delay measured between the peak of saturated head at the furthermost point and at the outlet of the hollow [*Montgomery et al.*, 1997, Figure 18]. Rainstorms with this intensity and duration have return periods $1/\lambda(h_{cr}) \approx 1400$ yrs (equation (7), with u = 4.23 mm h^{-1}, v = 1.62 mm h^{-1}), which are larger than T_{imm}. This regime can be defined as "event limited." Figure 5a shows how, due to the lower critical rainstorm frequency, mass-wasting processes are

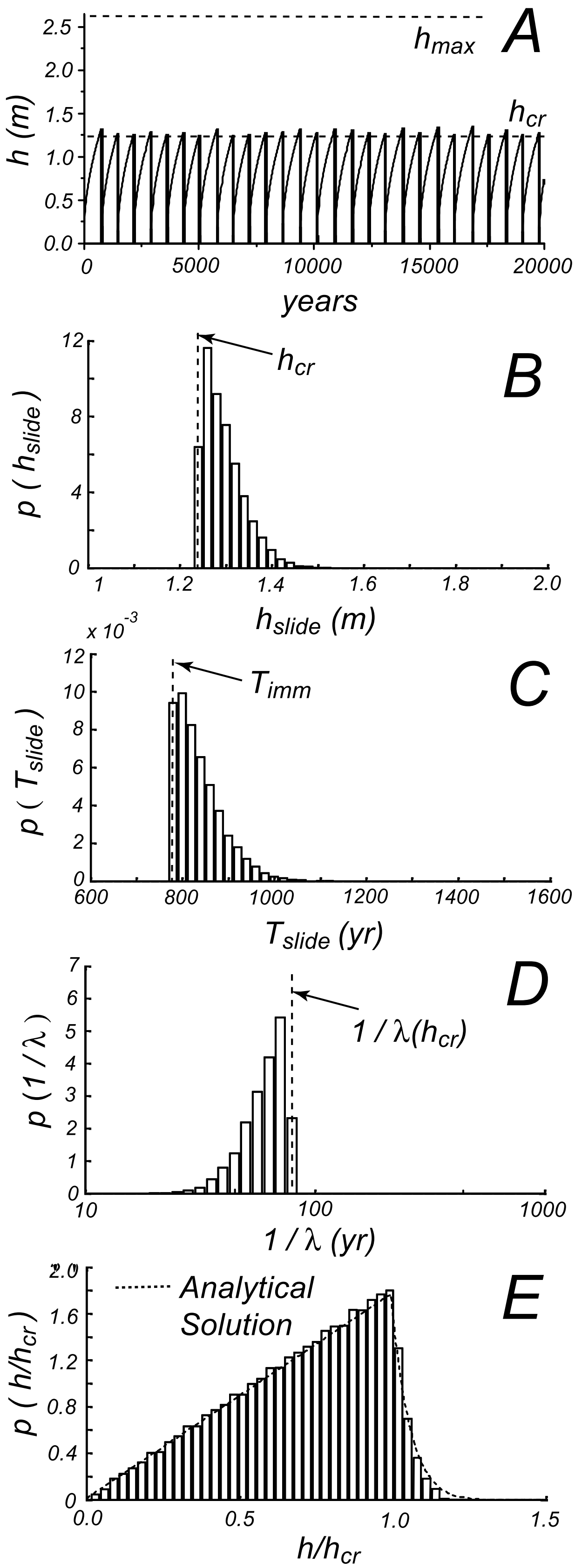

Figure 4. (opposite) Example of supply-limited processes in a steep hollow ($\beta = 43°$, $\phi = 33°$, $A = 3700$ m^2): (a) time series of deposit thickness; (b) probability distribution of scar depth (i.e., colluvium thickness when a landslide occurs); (c) probability distribution of landslide return period; (d) probability distribution of the return period of landslide-triggering storms ($1/\lambda(h_{slide})$); (e) probability distribution of colluvium thickness.

able to accumulate debris material in the hollow even when the deposit thickness is greater than the immunity depth. An increase in thickness makes the slope more prone to landsliding and reduces both intensity and return period of the triggering precipitation. In the limit, when $h = h_{max} = 2.66$ m, a landslide is triggered regardless of the rainfall. It will be shown that this is not the case on gentle slopes ($\beta < \phi$). Thus landslides occur when soil thickness is between h_{cr} and h_{max} (Figures 5a and 5b). The return period of the triggering rainfall ranges from 50 to 1400 yr (Figure 5d), and the return period of landsliding increases with respect to the case of Figure 4, while its probability distribution is sparser (Figure 5c). The mode of the probability distribution of soil thickness is no more coinciding with h_{cr} but is located between h_{cr} and h_{max} (Figure 5e). It should be noted that the study of these rare events using Gumbel distribution (equation (7)) with parameters estimated on the basis of a 50-yearlong observation is just an extrapolation. Nevertheless, it provides at least a qualitative indication of the conditions controlling the occurrence of event-limited and supply-limited regimes.

8.2. Case of Gently Sloped Hollows ($\beta < \phi$)

[28] In the last example we study a hollow with slope $\beta = 30°$, keeping the same soil hydraulic and strength characteristics as in the previous examples. As mentioned before, when $\beta < \phi$ an increase in colluvium thickness favors slope stability. Thus the likelihood of landslide occurrence is maximum when $h = h_{cr}$ and decreases for higher values of h. Different conditions can occur, which depend on the ratio between landslide return period at $h = h_{cr}$ and the length of the immunity period: (1) if $1/\lambda(h_{cr}) \ll T_{imm}$ the system is in a supply-limited regime with $h_{slide} \approx h_{cr}$ and $T_{slide} \approx T_{imm}$; (2) if $1/\lambda(h_{cr}) \gg T_{imm}$ the hollow can develop a thick enough colluvium to become stable with respect to (almost) any storm. This means that $T_{slide} \rightarrow \infty$ and that landslides (almost) never occur. This extreme condition of the event-limited case can be named "unconditionally stable"; (3) if $1/\lambda(h_{cr}) \approx T_{imm}$ the system can either be in a supply-limited or in an unconditionally stable state; however, once a transition into the unconditionally stable state takes place the system is not likely to return to a supply-limited regime.

[29] These different conditions can be obtained, for example, by changing the hollow contributing area, keeping the same soil properties as before. Figure 6 shows the probability distribution of deposit thickness, landslide frequency and depth for $A = 7500$ m^2 ($\lambda(h_{cr})T_{imm} = 0.025$). This case corresponds to supply-limited conditions, and the shape of the probability distribution of h resembles that in Figure 4e, with landslides occurring soon after the deposit thickness exceeds h_{cr} and $h_{slide} \approx h_{cr}$. The main difference

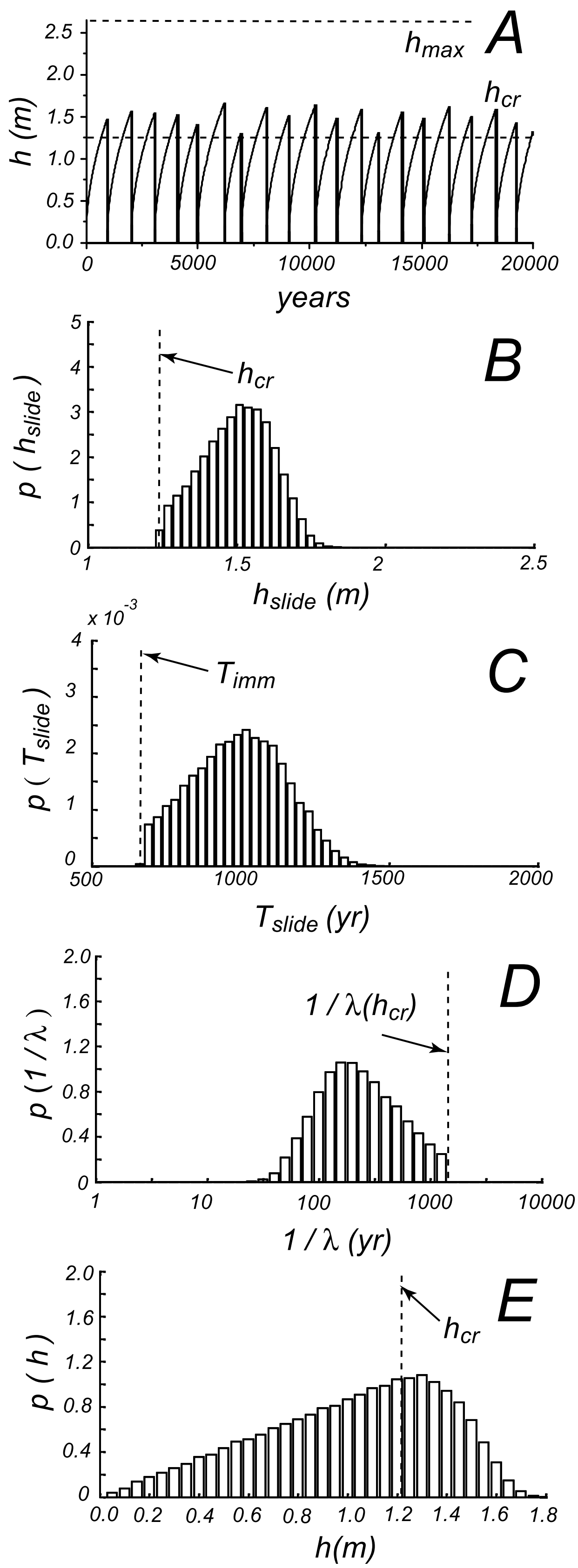

with respect to the supply-limited case of Figure 4 is that the return period of the storms generating landslides, $1/\lambda(h_{slide})$ is larger than $1/\lambda(h_{cr})$, due to the decrease of $\lambda(h)$ with increasing values of h in the case of gentle slopes. Figure 7 shows a case with A = 4500 m^2 ($\lambda(h_{cr})T_{imm} \approx 1$): this is an example of transition between supply-limited and unconditionally stable systems. When such a transition occurs there is little probability that the system is able to reverse into a event-limited state. It should be noted that some judgment is needed in the interpretation of the case of unconditionally stable systems: in fact this model does not account for the decrease of cohesion with increasing values of deposit thickness, due to the loss of the stabilizing effect of tree roots. Moreover, the downhill movement of soil waste material on gentle slopes does not necessarily occur as landsliding: other relatively slow processes (e.g., earth flow, mud flow, soil creep) characterize soil mass movement on gentler slopes [*Sidle et al.*, 1985]. These processes have not been included in our model.

[30] The results presented here can be extended to hollows with different geometric and hydrologic characteristics (reflected in different parameter sets) and to different conceptual models of hollow infilling and hydrologic response. Four different regimes may characterize the temporal evolution of colluvial deposits in hollows: the system can be supply limited ($1/\lambda(h_{cr}) \ll T_{imm}$) either on steep ($\beta > \phi$) or gentle slopes ($\beta < \phi$); otherwise, the dynamics are event-limited ($1/\lambda(h_{cr} \gg T_{imm})$ on steep or gentle (unconditionally stable) slopes. The attribution of a particular regime to a hollow only depends on the slope and on the ratio between the immunity period and the return period of the triggering precipitation associated with values of soil thickness equal to the immunity depth. These four regimes still exist when different hydrological models and hollow infilling schemes are used, as well as when soil production by weathering of the underling bedrock is added to sediment supply from the adjacent slopes (compare the models presented by *Dunne* [1991], *Montgomery and Dietrich* [1994], *Dietrich et al.* [1995], and *Iida* [1999]). These four regimes produce qualitatively similar results provided that (1) equation (1) is utilized to assess the slope stability, and (2) the hydrological model expresses the saturated depth as an increasing (linear) function of rainfall intensity.

8.3. Preferential States and Minima of the Potential Function

[31] The occurrence of supply-limited, event-limited, and unconditionally stable states can be studied through a potential function [e.g., *Hanggi et al.*, 1990; *Porrá and Masolivier*, 1993] associated to equations (11)–(13). The potential function is used to study some distinctive properties of the temporal dynamics of colluvial deposits and in particular to determine the preferential state(s) of the system

Figure 5. (opposite) Example of event-limited processes in a steep hollow ($\beta = 43°$, $\phi = 33°$, A = 860 m^2): (a) time series of deposit thickness; (b) probability distribution of scar depth (i.e., colluvium thickness when a landslide occurs); (c) probability distribution of landslide return period; (d) probability distribution of the return period of landslide-triggering storms ($1/\lambda(h_{slide})$); (e) probability distribution of colluvium thickness.

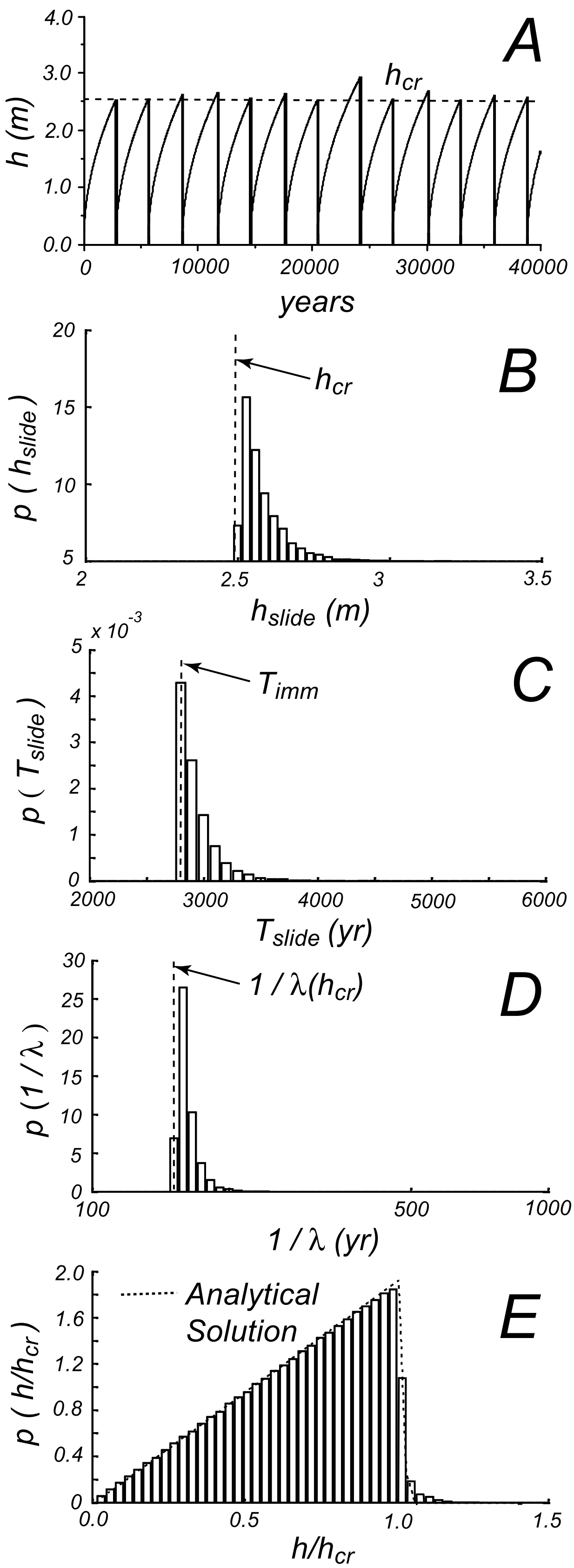

[*D'Odorico*, 2000; *D'Odorico et al.*, 2001]. Thus this framework points out some important properties of the evolution of colluvial deposits. Equation (11) can be rewritten as

$$\frac{dh}{dt} = -\frac{dV}{dh} - \xi(x, t) \tag{14}$$

where $\xi(x, t) = f(h, t) - \lambda(h)\omega(h)$ is a zero-average noise term (see equations (12) and (13)), while $V(h)$ is the potential function associated with the deterministic dynamics $\frac{dh}{dt} = l(h) + \lambda(h)\omega(h)$. The minima of this function represent stable states of the system: thus, in the absence of noise, h changes in time in the direction of decreasing values of $V(h)$ (Figure 8a) until it reaches a stable state. The noise moves the system away from the stable states and, in the case of multistable systems (i.e., with multiple preferential states as in Figure 8b), it can even move h to the basin of attraction of another stable state. The system is most likely to be found in the proximity of stable states and the corresponding values of h are closely associated with maxima (i.e., modes) of the probability distribution of h. In the study of hollow dynamics we are in particular interested in the analysis for $h > h_{cr}$ (for $h < h_{cr}$ the system undergoes a deterministic dynamics of soil accretion, with the potential function decreasing for $h \rightarrow h_{cr}$); the potential function can be expressed as

$$V(h) = -\int_{h_{cr}}^{h} [l(h) + \lambda(h)h]dh + const \qquad (h \geq h_{cr}) \tag{15}$$

where $\lambda(h)$ is expressed through equations (2), (5), (6), and (7).

[32] Figure 9 shows the potential functions of the examples discussed in the previous section. In the case of the hollow of Figure 4 the potential function (Figure 9a) shows a minimum at $h = h_{cr}$. This is the case of a supply-limited system, with a mode in the distribution of colluvium thickness coinciding with the immunity depth, which also represents the preferential state of the system. Landsliding in the hollow of Figure 5 is event-limited in the sense explained before. Landsliding occurs with soil depths larger than the immunity depth; there is a larger variance in the values of h_{slide} and T_{slide}. The mode in the distribution of h is between h_{cr} and h_{max} (in this example the mode is slightly above h_{cr}), coinciding with the position of the potential well in Figure 9b. The hollow discussed in Figure 6 is another example of supply-limited systems with both potential well and mode of h being at $h = h_{cr} = 2.51$ m (Figure 9c). The last example (Figure 7) is characterized by a potential

Figure 6. (opposite) Example of supply-limited processes in a gentle-slope hollow ($\beta = 30°$, $\phi = 33°$, $A = 7500$ m^2, $h_{cr} = 2.51$ m, $T_{imm} \approx 6{,}000$ yrs, $R(h_{cr}) = 5.5$ mm h^{-1}, $T_c = 24$ h, $u = 1.84$ mm h^{-1}, $v = 0.71$ mm h^{-1}, $1/\lambda(h_{cr}) \approx 160$ yrs): (a) time series of deposit thickness; (b) probability distribution of scar depth (i.e., colluvium thickness when a landslide occurs); (c) probability distribution of landslide return period; (d) probability distribution of the return period of landslide-triggering storms ($1/\lambda(h_{slide})$); (e) probability distribution of colluvium thickness.

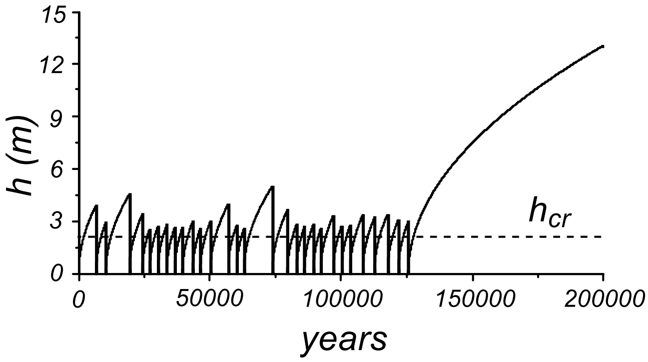

Figure 7. Example of transition from an event-limited state to an unconditionally stable state in the dynamics of a gentle-slope hollow ($\beta = 30°$, $\phi = 33°$, $A = 4500$ m^2, $h_{cr} = 2.51$ m, $T_{imm} \approx 6000$ yrs, $R(h_{cr}) = 9.1$ mm h^{-1}, $T_c = 18$ h, $u = 2.13$ mm h^{-1}, $v = 0.82$ mm h^{-1}, $1/\lambda(h_{cr}) \approx 5000$ yrs): time series of the deposit thickness.

function with two potential wells, one at h_{cr}, corresponding to a supply-limited regime, and the other at $h \to \infty$, corresponding to an unconditionally stable system; a potential barrier at $h = 3.5$ m separates the two regimes.

9. An Analytical Solution

[33] As mentioned before, according to this model, supply-limited conditions are common both in steep and in gentle-slope hollows. We suggest an analytical solution of the stochastic differential equation (11) that is valid for the case of λ independent of h. This condition is met in supply-limited systems, where landslides occur soon after the deposit depth exceeds h_{cr}; in this case the frequency of the triggering storm can be assumed constant and equal to $\lambda(h_{cr})$. Equations (11)–(13) can be written as a function of the dimensionless depth $\chi = h/h_{cr}$

$$\frac{d\chi}{dt} = \lambda L(\chi) - F(\chi, t) \qquad (16)$$

where $F(\chi, t) = \Omega(\chi)\Sigma_i\ \delta(t - t_i)$ and $L(\chi) = \frac{l(h)}{\lambda h_{cr}}$; with $\Omega(\chi) = \omega(h)/h_{cr}$. When the rate of colluvium accretion, $l(h)$, is given by (10), $L(\chi)$ becomes

$$L(\chi) = \frac{l(h)}{\lambda h_{cr}} = \frac{1}{2\zeta\chi} \qquad (17)$$

with $\zeta = \lambda h_{cr}^2/K$. The solution of (16) provides the probability density function of χ (see Appendix)

$$p(\chi) = \begin{cases} \dfrac{C}{L(\chi)}; & 0 \le \chi < 1 \\ \dfrac{C}{L(\chi)} e^{-\Theta(\chi)}; & \chi \ge 1 \end{cases} \qquad (18)$$

where

$$\Theta(\chi) = \int_1^{\chi} \frac{d\chi}{L(\chi)} = \zeta(\chi^2 - 1). \qquad (19)$$

and $C = \frac{1}{[1-\Theta(0)]} = \frac{1}{1+\zeta}$. It can be shown that $p(\chi)$ has only one mode value (at $\chi = 1$ when $\zeta \ge 0.5$, or at $\chi = \sqrt{1/(2\zeta)}$, when $\zeta < 0.5$).

[34] The average recurrence period, T_L, of landslides is

$$\lambda T_L = \frac{1}{p(0)\ L(0)} = 1 - \Theta(0) = 1 + \zeta; \qquad (20)$$

Thus the landslide return period, T_L, can be expressed as sum of the average time between two consecutive extreme rainstorms and the recovery time, T_{imm}, of the hollow, i.e., the time needed by the hollow to develop a deposit thickness from zero (immediately after a landslide) to the immunity depth

$$T_L = \frac{1}{\lambda} + T_{imm} = \frac{1}{\lambda} + \frac{h_{cr}^2}{K}; \qquad (21)$$

In equation (21) $\frac{1}{\lambda}$ depends on the hydro-climatic forcing, while T_{imm} depends on the parameters of the soil accretion function as well as on the immunity depth, hence on the slope and shear strength parameters.

[35] Figure 10 shows the probability distribution of the (normalized) regolith depth for different values of the dimensionless parameter $\zeta = \lambda h_{cr}^2/K$. The probability distribution is an increasing function of χ until $\chi = 1$; above this value, the behavior is twofold. If $\zeta > 1/2$ (i.e., $h_{cr} > \sqrt{K/(2\lambda)}$) the distribution decreases monotonically, whereas if $\zeta < 1/2$ (i.e., $h_{cr} < \sqrt{K/(2\lambda)}$) the distribution continues to increase until $\chi = \sqrt{1/(2\zeta)}$ and it decreases for larger values of χ. This difference reflects the distinction between event-limited and supply-limited systems, dis-

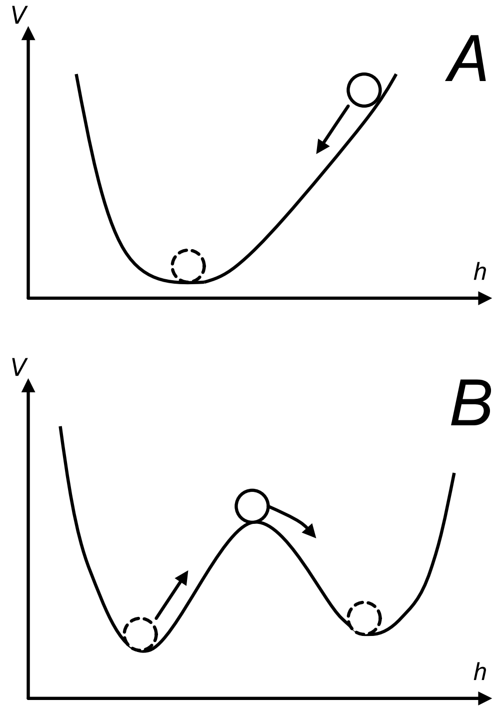

Figure 8. Schematic representation of (a) system evolution toward its potential well; (b) bistable system with a noise-induced transition from a potential well to another.

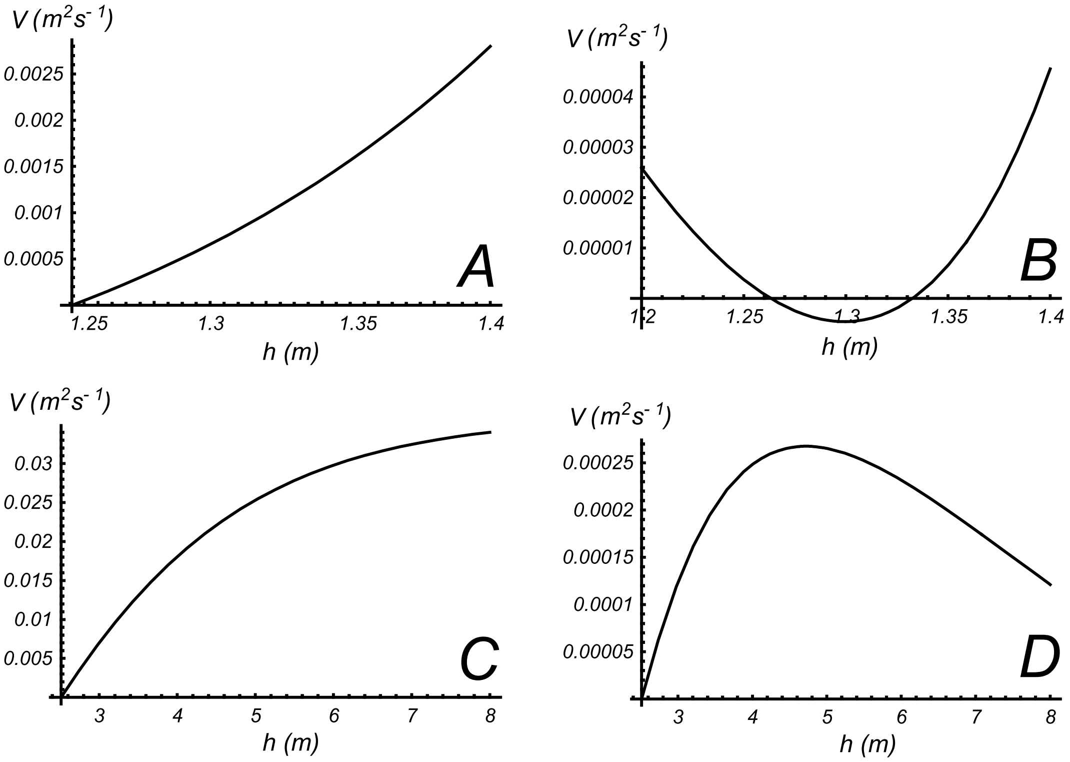

Figure 9. Potential function for the hollows of (a) Figure 4 (supply limited); (b) Figure 5 (event limited); (c) Figure 6 (supply limited); (d) Figure 7 (bistable system).

cussed before. For $\zeta > 1/2$, the mode of the distribution of soil thickness is $\chi = 1$ (i.e., $h = h_{cr}$) and the system is in a supply-limited condition; in this case the analytical solution (18) can be properly applied and it can be favorably compared with the numerical results determined for the examples analyzed in Figures 4 and 6. On the other hand, in the event-limited condition, the analytical solution cannot be applied since λ strongly depends on the soil thickness h.

[36] The probability distribution of χ can be used to estimate the average (normalized) thickness of the regolith and to assess its dependence on immunity depth, slope angle and soil strength parameters

$$\langle\chi\rangle = \int_0^\infty \chi p(\chi)\, d\chi = \frac{2\zeta}{1+\zeta}\left[\frac{1}{3}+\frac{1}{2\zeta}+\frac{\sqrt{\pi}e^{\zeta}}{4\zeta^{3/2}}\left(1-Erf\left(\sqrt{\zeta}\right)\right)\right]. \qquad (22)$$

With the higher values of ζ (i.e., of the ratio between rate of landslide occurrence and rate of deposit accretion) the long-term average soil depth, $\langle\chi\rangle$, is smaller (equation (22)) because landslides occur before the hollow is able to develop thick deposits. This means that, with a given h_{cr}, large rates of transport (with respect to the rates of deposit accretion) correspond to smaller values of $\langle\chi\rangle$. The standard deviation, σ, of χ is also a decreasing function of ζ. In fact, large values of λ correspond to a supply-limited process where landslides occur when $h = h_{cr}$; this limits most of the variability of h within the interval $(0, h_{cr})$ (i.e., of χ in (0,1)) and the variance is contributed mostly by the variability in the course of the immunity period (i.e., $0 \leq h \leq h_{cr}$ or $0 \leq \chi \leq 1$).

10. Conclusions

[37] A stochastic (process-based) model has been suggested for the study of the temporal evolution of regolith thickness in a hollow. The model consists of a soil mass balance equation with a deterministic representation of the mechanisms of soil accumulation in the hollow due to transport of soil from the lateral hillslopes, and of their dependence on the thickness of the deposit. The erosion of the soil mantle due to landslides is modeled as a stochastic

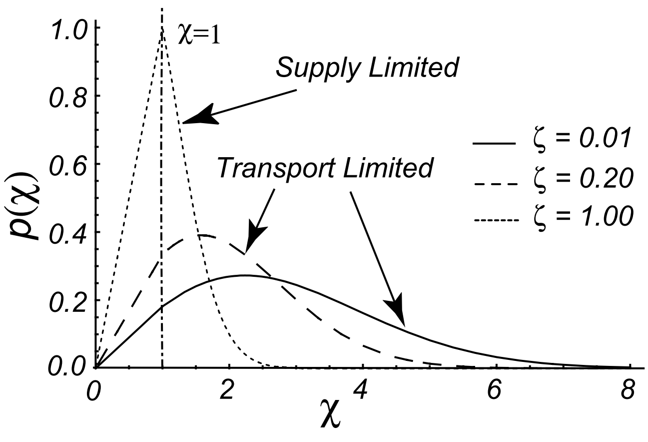

Figure 10. Probability distribution of the (normalized) soil thickness, $\chi = h/h_{cr}$, for different values of ζ.

(Poisson) process, with each landslide removing the whole hollow fill. Landslides do not occur when the colluvium thickness is less than the immunity depth; the latter depends on the hollow slope and soil mechanical properties. Landslide frequency is linked to the rainfall intensity-duration-frequency curves through a hydrological model. This framework relates landslide return period to the rainstorm frequency and to the rate of hollow recovery after a landslide.

[38] This analysis has shown that (1) for hollow slope, β, greater than the colluvium repose angle, ϕ, an increase in soil thickness favors instability, reducing the rain intensity necessary to trigger a landslide. It is then possible to define a maximum soil thickness h_{max}, above which a landslide would occur, even in the absence of rainfall. Thus landslides always occur when the soil thickness is between the immunity depth and h_{max}. Conversely, when $\beta < \phi$, an increase in soil thickness leads to an increase in the landslide-triggering rainfall intensity, favoring the stability of the hollow. (2) In the case of $\beta > \phi$ two possible regimes are identified depending on the ratio between the immunity period (i.e., time needed by the hollow to fill up to the immunity depth), T_{imm}, and the return period, $1/\lambda(h_{cr})$, of the landslide-triggering rainfall when the soil thickness is equal to the immunity depth. If $1/\lambda(h_{cr}) \ll T_{imm}$ the accumulation of material in the hollow is slow compared to the time elapsing between two consecutive triggering rainstorms. In this case, landslides occur soon after the deposit thickness reaches the immunity depth and the return period of landsliding is close to the immunity period, while the return period of the triggering rainfall is approximately $1/\lambda(h_{cr})$. Landslide occurrence is limited by the supply of debris from the adjacent slopes and not by the occurrence of triggering precipitation: we denote this regime as "supply limited". Vice versa, if $1/\lambda(h_{cr}) \gg T_{imm}$ only rare (i.e., intense) rainstorms are able to trigger a landslide when $h = h_{cr}$. This means that the colluvium thickness can significantly increase above the immunity depth before the occurrence of landslides; this growth of colluvial deposits in steep hollows is accompanied by an increase in the hollow susceptibility to landsliding (see point 1). The probability distribution of landslide return period, as well as of the return period of the triggering rainfall and of the scar thickness, strongly depend on the statistics of extreme rainfall. The regime can be denoted as "event limited" because landsliding is limited by the occurrence of the triggering precipitation. (3) Two more regimes can be similarly defined in the case of gentle slopes ($\beta < \phi$): when $1/\lambda(h_{cr}) \ll T_{imm}$ the hollow is in supply-limited condition, with rainfalls triggering landslides soon after the deposit depth reaches h_{cr}. When $1/\lambda(h_{cr}) \ll T_{imm}$ the triggering precipitation is characterized by high return periods; therefore the deposit accretion is likely to exceed the immunity depth. The stability of the hollow increases with the deposit thickness until the slope is no more prone to hydrologically triggered landslides. This regime is here defined as "unconditionally stable."

[39] The analysis is further carried out with the introduction of a potential function, that allows the identification of stable equilibrium configurations (corresponding to potential minima). If the system is characterized by more than one stable configuration, the random forcing associated with the stochastic representation of precipitation can lead to the transition from a potential minimum to another. The analysis of the potential function agrees with results of the stochastic soil mass balance model. For example, in supply-limited conditions, there is a minimum at $h = h_{cr}$, whereas in the case of transition from supply-limited to unconditionally stable there exist two minima, one at $h = h_{cr}$ and the other at $h \rightarrow \infty$, representing an unconditionally stable state.

[40] Furthermore, in the case of supply-limited conditions, an analytical solution is derived from the stochastic soil mass balance equation, considering a constant landslide return period equal to the immunity period. This solution well matches the numerical results. The supply-limited condition produces a periodic delivery of sediments to the channel network, with little variation in return period and debris volume. Hollows less prone to landsliding, instead, deliver material with a more variable return period and debris volume, depending on the rainfall regime.

Appendix A

[41] The analytical solution of the stochastic differential equations (10)–(11) can be constructed using the same approach as by *Cox and Miller* [1965], *Cox and Isham* [1986], and *Rodriguez-Iturbe et al.* [1999].

[42] The rate, λ, of occurrence of the climatic forcing is assumed to be independent of the thickness of the colluvial deposit; nevertheless, due the existence of the immunity depth, the rate of occurrence of landslides differs from λ and depends on the depth of the deposit. When soil depth is less than h_{cr} the occurrence of a triggering event does not result in any soil removal. The probability distribution of the amount of soil removed, ω (equation (13)), is therefore a Dirac delta-function centered on 0 (i.e., $\delta(\omega)$). When soil depth is greater than h_{cr} all soil is removed. The probability distribution of landslide thickness is therefore a Dirac delta function centered on h (i.e., $\delta(\omega - h)$). The combined depth-dependent probability distribution of the amount of soil removed is therefore

$$p(\omega) = \begin{cases} \delta(\omega); & 0 < h < h_{cr} \\ \delta(\omega - h); & h_{cr} \leq h \end{cases} \tag{A1}$$

[43] In the interval $(t, t + \Delta t)$ there is a probability $(1 - \lambda\Delta t)$ that no landslide occur and that the deposit depth at time $t + \Delta t$ is $h(t + \Delta t) = h(t) + \Delta h(t)$, while with probability $\lambda\Delta t$ a landslide of depth ω occurs and at time $t + \Delta t$ the deposit depth is $h(t + \Delta t) = h(t) + \Delta h(t) - \omega$.

[44] The probability of having a deposit thickness, h, at time $t + \Delta t$ is separately estimated for the cases $h < h_{cr}$ and $h \geq h_{cr}$

$$p(h, t + \Delta t)\Delta h(h)$$

$$= \begin{cases} p(h - \Delta h, t)(1 - \lambda\Delta t)\ \Delta h(h - \Delta h) + \\ p(h - \Delta h + \omega, t)\lambda\Delta t\ \Delta h(h - \Delta h); \\ \qquad\qquad (0 < h < h_{cr}) \\ p(h - \Delta h, t)(1 - \lambda\Delta t)\ \Delta h(h - \Delta h); \\ \qquad\qquad (h \geq h_{cr}) \end{cases} \tag{A2}$$

where, in the first equation, $\omega = 0$ because $h < h_{cr}$ (equation (13)), while the second equation has been obtained observing that the deposit thickness at time $t + \Delta t$ is h only if it is $h - \Delta h$ at time t and no landslides occur. After a Taylor expansion about (h, t), expressing Δh as $l(h)\Delta t$, and dividing by $\Delta h\ \Delta t$, the above becomes

$$\frac{\partial p(h;t)}{\partial t} = \begin{cases} -\dfrac{\partial}{\partial h}[p(h;t)\ l(h)]; & 0 < h < h_{cr} \\ -\dfrac{\partial}{\partial h}[p(h;t)\ l(h)] - \lambda p(h;t); & h \geq h_{cr} \end{cases} \tag{A3}$$

[45] The probability that $h = 0$ at time $t + \Delta t$ is the probability that $h \geq h_{cr}$ at time t and that a landslide occurs in the interval (t, $t + \Delta t$); hence

$$p(0)\ l(0) = \lambda \int_{h_{cr}}^{\infty} p(h')\ dh' \tag{A4}$$

and this is also the probability of landslide occurrence.

[46] Equations (A3) and (A4) provide a piecewise representation of the master equation [*Cox and Miller*, 1965] for $0 < h < h_{cr}$, $h \geq h_{cr}$, and $h = 0$, respectively. In statistically steady state conditions ($t \to \infty$) the temporal derivatives are null and equations (A3) become

$$\frac{d}{dh}[p(h)l(h)] = 0; \qquad 0 \leq h < h_{cr} \tag{A5a}$$

$$\frac{d}{dh}[p(h)l(h)] = -\lambda p(h); \qquad h \geq h_{cr} \tag{A5b}$$

with the boundary condition (A4).

[47] The integration of the system (A5a) leads to two algebraic equations with two integration constants that are estimated through the imposition of two conditions: the normalization of $p(h)$ (i.e., unit value of the integral of $p(h)$ in the interval $[0, +\infty)$) and equation (A4) granting the continuity of the dynamics between $h = 0$ and $h > 0$ (in fact the soil depth continuously grows from $h = 0$ to values of h larger than zero; thus equation (A4) represents the boundary condition for (A5a) leading to

$$p(h)l(h) = \lambda \int_{h_{cr}}^{\infty} p(h)dh (0 \leq h < h_{cr}). \tag{A6}$$

[48] At the same time, the integration of (A5b) gives

$$p(h) = \frac{C}{l(h)} e^{-\lambda \int_{h_{cr}}^{h} \frac{dh'}{l(h')}} = -\frac{C}{\lambda}\frac{d}{dh}\left[e^{-\lambda \int_{h_{cr}}^{h} \frac{dh'}{l(h')}}\right];\ (h \geq h_{cr}) \tag{A7}$$

where C is an integration constant.

[49] Using (A7), equation (A6) becomes

$$p(h) = \frac{C}{l(h)}\left[1 - e^{-\lambda \int_{h_{cr}}^{\infty} \frac{dh'}{l(h')}}\right](0 \leq h < h_{cr}). \tag{A8}$$

[50] The probability density function of h finally reads as

$$p(h) = \begin{cases} \dfrac{C}{l(h)}\left(1 - e^{-\theta(\infty)}\right); & 0 < h_{cr} \\ \dfrac{c}{l(h)} e^{-\theta(h)}; & h \geq h_{cr} \end{cases} \tag{A9}$$

where: $\theta(h) = \lambda \int_{h_{cr}}^{h} \frac{dx}{l(x)}$. The constant C is found by normalization (i.e., $\int_0^{\infty} p(h)\ dh = 1$), leading to: $C = \frac{\lambda}{[1-\theta(0)]}$. In particular, it can be shown that, when $l(h)$ is expressed by (10), $\exp(-\theta(h)) = 0$ for $h \to \infty$, while $\exp(-\theta(h)) = 1$ for $h = h_{cr}$. This grants the continuity of $p(h)$ at $h = h_{cr}$.

[51] **Acknowledgments.** This paper has greatly benefited from the comments of three anonymous referees and an associate editor, who reviewed a previous version of this manuscript. We gratefully acknowledge the contribution of Amilcare Porporato (Polytechnic of Turin) to the development of the analytical solution.

References

Ahnert, F., Modelling landform change, in *Modelling Geomorphological Systems*, edited by M. G. Anderson, pp. 375–400, John Wiley, Hoboken, N. J., 1988.

Anderson, S. P., W. E. Dietrich, D. R. Montgomery, R. Torres, M. E. Conrad, and K. Loague, Subsurface flow paths in a steep, unchanneled catchment, *Water Resour. Res.*, *33*, 2637–2653, 1997.

Anderson, S. P., W. E. Dietrich, and G. H. Brimhall, Weathering profiles, mass-balance analysis, and rates of solute loss: Linkages between weathering and erosion in a small, steep catchment, *Geol. Soc. Am. Bull.*, *114*(9), 1143–1158, 2002.

Benda, L., and T. Dunne, Stochastic forcing of sediment supply to channel networks from landsliding and debris flow, *Water Resour. Res.*, *33*, 2849–2863, 1997.

Birkeland, P. W., *Soils and Geomorphology*, Oxford Univ. Press, New York, 1999.

Caine, N., The rainfall intensity-duration control of shallow landslides and debris flows, *Geograf. Ann. A.*, *62*, 23–27, 1980.

Carson, M. A., and M. J. Kirkby, *Hillslope Form and Process*, Cambridge Univ. Press, New York, 1972.

Chow, W. T., D. R. Maidment, and L. W. Mays, *Applied Hydrology*, McGraw-Hill, New York, 1988.

Cox, D. R., and V. Isham, The virtual waiting-time and related processes, *Adv. Appl. Prob.*, *19*, 558–573, 1986.

Cox, D. R., and H. D. Miller, *The Theory of Stochastic Processes*, John Wiley, Hoboken, N. J., 1965.

Crozier, M. J., E. E. Vaughan, and J. M. Tippett, Relative instability of colluvium-filled bedrock depressions, *Earth Surf. Processes Landforms*, *15*, 329–339, 1990.

Culling, W. E. H., Analytical theory of erosion, *J. Geol.*, *68*(3), 336–344, 1960.

Dietrich, W. E., C. J. Wilson, and S. L. Reneau, Hollows, colluvium, and landslides in soil-mantled landscapes, in *Hillslope Processes*, edited by A. D. Abrahams, pp. 361–388, Allen and Unwin, Concord, Mass., 1986.

Dietrich, W. E., S. L. Reneau, and C. J. Wilson, Overview: "zero-order basins" and problems of drainage density, sediment transport and hillslope morphology, in *Erosion and Sedimentation in the Pacific Rim*, edited by R. L. Beschta, *IAHS Publ.*, *165*, 27–37, 1987.

Dietrich, W. E., R. Reiss, M. L. Hsu, and D. Montgomery, A process-based model for colluvial soil depth and shallow landslides using digital elevation data, *Hydrol. Processes*, *9*, 383–400, 1995.

D'Odorico, P., A possible bistable evolution of soil thickness, *J. Geophys. Res.*, *105*(B11), 25,927–25,935, 2000.

D'Odorico, P., A. Porporato, and L. Ridolfi, Transition between stable states in the dynamics of soil development, *Geophys. Res. Lett.*, *28*(4), 595–598, 2001.

Dunne, T., Stochastic aspects of the relations between climate, hydrology and landform evolution, *Trans. Jpn. Geomorphol. Union*, *12*, 1–24, 1991.

Eagleson, P. S., Climate, soil, and vegetation: 2. The distribution of annual precipitation derived from observed storm sequences, *Water Resour. Res.*, *14*, 713–721, 1978.

Furbish, D. J., and S. Fagherazzi, Stability of creeping soil and implications for hillslope evolution, *Water Resour. Res.*, *37*, 2607–2618, 2001.

Hanggi, P., P. Talkner, and M. Borkovec, Reaction-rate theory: Fifty years after Kramers, *Rev. Mod. Phys.*, *62*, 251–342, 1990.

Heimsath, A. M., W. E. Dietrich, K. Nishiizumi, and R. C. Finkel, The soil production function and landscape equilibrium, *Nature*, *388*, 358–361, 1997.

Heimsath, A. M., W. E. Dietrich, K. Nishiizumi, and R. C. Finkel, Stochastic processes of soil production and transport: Erosion rates, topographic variation and cosmogenic nuclides in the Oregon Coast Range, *Earth Surf. Proc. Landforms*, *26*, 531–552, 2001.

Iida, T., A stochastic hydro-geomorphological model for shallow landsliding due to rainstorm, *Catena*, *34*(3–4), 293–313, 1999.

Iverson, R. M., Landslide triggering by rain infiltration, *Water Resour. Res.*, *36*, 1897–1910, 2000.

Kirkby, M. J., Hillslope process-response models based on the continuity equation, in *Slopes, Form, and Process*, *Spec. Publ.*, vol. 3, pp. 15–30, Inst. of Br. Geogr., London, 1971.

Lancaster, S. T., S. K. Hayes, and G. E. Grant, Modeling sediment and wood storage dynamics in small mountainous watersheds, in *Geomorphic Processes and Riverine Habitat*, *Water Sci. Appl. Ser.*, vol. 4, edited by B. P. J. Dorava et al., pp. 85–102, AGU, Washington, D. C., 2001.

Minasny, B., and A. B. McBratney, A rudimentary mechanistic model for soil production and landscape development, *Geoderma*, *90*, 3–21, 1999.

Montgomery, D. R., and W. E. Dietrich, A physically-based model for the topographic control on shallow landsliding, *Water Resour. Res.*, *30*, 1153–1171, 1994.

Montgomery, D. R., W. E. Dietrich, R. Torres, S. P. Anderson, J. T. Heffner, and K. Loague, Hydrologic response of a steep, unchanneled valley to natural and applied rainfall, *Water Resour. Res.*, *33*, 91–109, 1997.

Montgomrery, D. R., K. Sullivan, and H. M. Greenberg, Regional test of a model for shallow landsliding, *Hydrol. Processes*, *12*, 943–955, 1998.

O'Loughlin, C. L., and A. J. Pearce, Influence of Cenozoic geology on mass movement and sediment yield response to forest removal, North Westland, New Zealand, *Bull. Int. Assoc. Eng. Geol.*, *14*, 41–46, 1976.

O'Loughlin, E. M., Prediction of surface saturation zones in natural catchments by topographic analysis, *Water Resour. Res.*, *22*, 794–804, 1986.

Porrà, J. M., and J. Masolivier, Bistability driven by white shot noise, *Phys. Rev. E*, *47*(3), 1633–1641, 1993.

Reneau, S. L., and W. E. Dietrich, Size and location of colluvial landslides in a steep forested landscape, in *Erosion and Sedimentation in the Pacific Rim*, edited by R. L. Beschta et al., *IAHS Publ.*, *165*, 39–48, 1987.

Reneau, S. L., W. E. Dietrich, M. Rubin, D. J. Donahue, and A. J. T. Jull, Analysis of hillslope erosion rates using dated colluvial deposits, *J. Geol.*, *97*, 45–63, 1989.

Rodriguez-Iturbe, I., A. Porporato, L. Ridolfi, V. Isham, and D. R. Cox, Probabilistic modelling of water balance at a point: The role of climate, soil and vegetation, *Proc. R. Soc. London, Ser. A*, *455*, 3789–3805, 1999.

Roering, J. J., J. W. Kirchner, and W. E. Dietrich, Evidence for non-linear, diffusive sediment transport on hillslopes and implications for landscape morphology, *Water Resour. Res*, *35*, 853–870, 1999.

Selby, M. J., *Hillslope Materials and Processes*, Oxford Univ. Press, New York, 1983.

Sidle, R. C., A dynamic model of slope stability in zero-order basins, in *Erosion and Sedimentation in the Pacific Rim*, edited by R. L. Beschta et al., *IAHS Publ.*, *165*, 101–110, 1987.

Sidle, R. C., and D. N. Swanston, Analysis of a small debris slide in coastal Alaska, *Can. Geotech. J.*, *19*, 167–174, 1982.

Sidle, R. C., A. J. Pearce, and C. L. O'Loughlin, *Hillslope Stability and Land Use*, *Water Resour. Monogr. Ser.*, vol. 11, AGU, Washington, D. C., 1985.

Terzaghi, K., and R. B. Peck, *Soil Mechanics in Engineering Practice*, Wiley Intersci., Hoboken, N. J., 1967.

Torres, R., W. E. Dietrich, D. R. Montgomery, S. P. Anderson, and K. Loague, Unsaturated zone processes and the hydrologic response of a steep, unchanneled catchment, *Water Resour. Res.*, *34*, 1865–1879, 1998.

Trustrum, N. A., and R. C. De Rose, Soil depth-age relationship of landslides on deforested hillslopes, Taranaki, New Zeland, *Geomorphology*, *1*, 143–160, 1988.

Tucker, G. E., and R. L. Bras, A stochastic approach to modeling the role of rainfall variability in drainage basin evolution, *Water Resour. Res.*, *36*, 1953–1964, 2000.

Tucker, G. E., S. T. Lancaster, N. M. Gasparini, and R. L. Bras, The channel-hillslope integrated landscape development (CHILD) model, *Landscape Erosion and Evolution Modeling*, edited by R. S. Harmon and W. W. Doe, III, pp. 349–388, Kluwer Acad., Norwell, Mass., 2001.

Wu, T. H., and D. N. Swanston, Risk of landslides in shallow soils and its relation to clearcutting in southeastern Alaska, *For. Sci.*, *26*(3), 495–510, 1980.

Wu, T. H., W. P. McKinnel, and D. N. Swanston, Strength of tree-roots and landslides on Prince of Wales Island, Alaska, *Can. Geotech. J.*, *16*(1), 19–33, 1979.

P. D'Odorico, Department Environmental Sciences, University of Virginia, Box 400123, Charlottesville, VA 22904-4123, USA. (paolo@virginia.edu)

S. Fagherazzi, Computational Science and Information Technology, Dirac Library Center, Tallahassee, FL 32306-4120, USA. (sergio@csit.fsu.edu)